Identification of Histidine 25 as the Heme Ligand in Human Liver Heme Oxygenase†

Jie Sun and Thomas M. Loehr*

Department of Chemistry, Biochemistry, & Molecular Biology, Oregon Graduate Institute of Science & Technology, P.O. Box 91000, Portland, Oregon 97291-1000

Angela Wilks and Paul R. Ortiz de Montellano

Department of Pharmaceutical Chemistry, School of Pharmacy and Liver Center, University of California, San Francisco, California 94143-0446

Received July 20, 1994®

ABSTRACT: Electronic and resonance Raman spectroscopic studies are reported for the His25Ala mutant of human liver heme oxygenase (HO) and its complex with heme. In the oxidized (ferric) form of the enzyme·substrate complex, the heme is shown to be in a high-spin, five-coordinate state. This is distinct from the same complex in the wild-type enzyme in which the heme is six-coordinate, ligated to a proximal histidine and a water molecule in an environment reminiscent of aquometmyoglobin. The reduced (ferrous) form of the complex of the H25A heme oxygenase mutant has lost the very prominent resonance Raman band at ~217 cm^{-1} seen in the wild-type complex that has been unambiguously assigned to the proximal Fe−N(His) vibrational frequency [Sun et al. (1993) *Biochemistry 32*, 14151; Takahashi et al. (1994) *Biochemistry 33*, 1010]. The absence of this band in the spectrum of the mutant protein definitively identifies His 25 as the proximal ligand of the heme substrate. Furthermore, this ferrous heme−H25A HO complex exists as an equilibrium mixture between a five-coordinate, high-spin species and a four-coordinate, intermediate-spin species. Although the H25A mutant protein shows no heme oxygenase activity, the heme is competent to bind carbon monoxide. Studies of the CO adduct of the H25A HO complex show ν(CO) and ν(Fe−CO) frequencies at 1960 and 529 cm^{-1}, respectively, that are characteristic of a hydrophobic carbon monoxide binding site on a heme with a weak proximal ligand. Furthermore, these frequencies indicate that the ligand trans to the CO in the adduct cannot be a histidine, a result that is entirely consistent with the absence of the His 25 ligand in the enzyme with the point mutation. The fifth ligand in the ferric and ferrous forms of the heme−H25A HO is ruled out as being from another histidine or a tyrosine. However, the exact identity of the weak ligand as well as the site of attachment (proximal versus distal, relative to the wild type enzyme) are not known at the present time.

Heme oxygenase catalyzes the conversion of the heme macrocycle to open chain biliverdin by elimination of the α-meso carbon as CO (Tenhunen et al., 1969; Maines, 1992). Recently, heme oxygenase activity in the brain has been implicated in the role of CO as a neural messenger (Stevens & Wang, 1993; Verma et al., 1993; Zhuo et al., 1993). This enzyme has been purified from several sources, including rat liver (Yoshida & Kikuchi, 1979), pig spleen (Yoshida & Kikuchi, 1978), bovine spleen (Yoshinaga et al., 1982), and chicken liver (Bonkovsky et al., 1990). Two isozymes encoded by two different genes, HO-1 and HO-2,[1] have been identified (Shibahara et al., 1985; Maines et al., 1986; Maines, 1988; Yoshida et al., 1988; Evans et al., 1991). A soluble, fully active rat liver enzyme (rHO-1C$^-$), truncated by 23 C-terminal amino acids, has been expressed and purified in our laboratory (Wilks & Ortiz de Montellano, 1993). Using resonance Raman and EPR studies on rHO-1C$^-$, we have established that heme oxygenase binds heme substrate by forming a proximal histidine linkage (Sun et al., 1993). The heme−heme oxygenase complex thus formed has spectroscopic properties similar to those of myoglobin. In the ferric form, the iron is also bound to a distal H_2O molecule and is, therefore, in a six-coordinate, high-spin state. This H_2O ionizes at pH ~8 to give hydroxo species in a high-spin/low-spin mixture, or it can be replaced by CN^- to yield a six-coordinate, low-spin cyano adduct. Our data also suggested that oxygen activation during heme degradation is mostly achieved by the distal heme pocket, with little aid from the proximal neutral histidine (Sun et al., 1993). Many of our observations have been independently corroborated and, in some cases, extended by more recent resonance Raman studies (Takahashi et al., 1994a,b). New NMR studies also suggest that the active-site pocket in the substrate-bound complex is very open. In addition, these studies suggest that the carboxylate side chain of an Asp or Glu appears to be located over the α-meso carbon of the heme to direct the specific attack at this position during the catalytic reaction (Hernández et al., 1994).

† This work was supported by grants from the U.S. Public Health Service, National Institutes of Health: GM34468 (T.M.L.) and DK30297 and GM32488 (P.R.O.d.M.).

* Author to whom correspondence should be addressed.

® Abstract published in *Advance ACS Abstracts,* October 15, 1994.

[1] Abbreviations: HO-1 and HO-2, different isozymes of heme oxygenase. HO-1C$^-$ denotes the deletion of 23 C-terminal amino acids from HO-1, giving a fully functional, soluble enzyme. hHO-1C$^-$ and rHO-1C$^-$ refer to the origin of the genes from human and rat liver, respectively, which were expressed in *Escherichia coli* to yield the proteins used in these studies.

0006-2960/94/0433-13734$04.50/0

Nonetheless, detailed information about the heme pocket that is necessary toward developing a mechanistic understanding is still lacking. Point mutagenesis studies have shown that, of the four fully conserved histidine residues, only His 25 and His 132 (rat liver HO-1 sequence) are essential to the enzyme activity (McCoubrey & Maines, 1993; Ishikawa et al., 1992). A more recent mutagenesis study, however, indicates that His 132 is essential for HO-2 but not for HO-1 heme oxygenase activity (Takahashi et al., 1994a). It is not clear which histidine functions as the proximal ligand in heme oxygenase. We have now succeeded in expressing and purifying a soluble, fully active truncated human liver HO-1 enzyme (hHO-1C$^-$) and its mutant His25Ala (Wilks and Ortiz de Montellano, manuscript in preparation). Here, we present spectroscopic evidence that His 25 is the proximal ligand in the heme−heme oxygenase complex of the hHO-1C$^-$ enzyme. This information now also allows us to suggest that His 132 is a functionally critical residue in the distal heme pocket.

MATERIALS AND METHODS

Heme oxygenase apoenzyme hHO-1C$^-$ and its mutant His25Ala, as well as their corresponding heme complexes, have been purified to homogeneity according to procedures to be described elsewhere (Wilks and Ortiz de Montellano, in preparation). The inactive heme complex samples, as purified (~100 μM), were in 10 mM potassium phosphate buffer (pH 7.4). They were used directly or further concentrated to ~300 μM through ultracentrifugation (Centricon). Change of pH was achieved either with 20 mM MES (pH 6.0) or with CAPS (pH 10.0) by two cycles of dilution (~10-fold) and reconcentration. Reduction of the heme to the ferrous state in these two complexes was achieved by adding a minimum amount of 100 mM sodium dithionite solution (in the appropriate buffer) to Ar-purged samples, and the progress was monitored by UV−vis spectroscopy. Exposure of the reduced samples to CO leads to the formation of carbonmonoxy adducts. For resonance Raman experiments (Loehr & Sanders-Loehr, 1993), a Spectra-Physics 2025-11 Kr^+ laser, a Spectra-Physics 164 Ar^+ laser, a Coherent INNOVA 90-6 Ar^+ laser, and a Liconix He-Cd 4240NB laser were used as excitation sources. Laser power at the sample was typically ~20 mW for excitation at 413.1 and 441.6 nm, and ~45 mW for longer wavelengths. [For the study of the carbonmonoxy adduct of the heme−His25Ala complex, low laser power (~2 mW, defocused) was used because of its sensitivity to photodissociation.] The enzyme samples in capillary tubes were placed in a metal rod cold finger which was immersed in an ice/water bath (90° scattering geometry). The scattered light was collected with either a DILOR Z24 Raman spectrophotometer having a thermoelectrically cooled (−40 °C) Hamamatsu 943-02 photomultiplier or a modified 25-300 Jarrell-Ash Raman spectrophotometer (cooled RCA C31034 photomultiplier). Signal-to-noise was enhanced by repetitive scanning on the same samples. Spectral resolution was typically ~5 cm^{-1}. UV−vis spectra were also monitored in the same capillary tubes used for the resonance Raman measurements (Loehr & Sanders-Loehr, 1993). FT-IR spectra of the CO adduct of the heme−H25A heme oxygenase complex (~300 μM) were obtained on a Perkin-Elmer Model 1800 instrument using a CaF_2 cell with a 35-μm spacer and collecting 200 scans. All the spectra were analyzed and processed with LabCalc (Galactic Industries, Salem, NH) on 486 PCs.

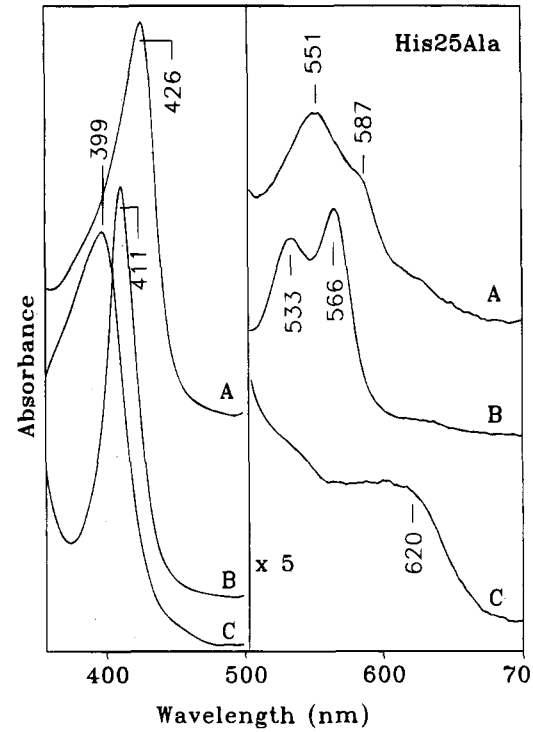

FIGURE 1: UV−vis spectra of the FePP−His25Ala hHO-1C$^-$ at pH 7.4 (~100 μM in capillary tubes). (A) Ferrous enzyme obtained by anaerobic reduction with sodium dithionite. (B) CO adduct of the ferrous enzyme. (C) Ferric enzyme.

RESULTS AND DISCUSSION

(A) UV−Vis Spectroscopy. The UV−vis spectra (ferrous, ferric) of the heme−hHO-1C$^-$ complex resemble those of the heme−rHO-1C$^-$ complex and are typical of hemes with a proximal histidine ligation (data not shown). The UV−vis spectra of heme substrate complexes of the H25A mutant protein are significantly different and are shown in Figure 1. The Soret absorption maxima of these complexes are at 426 nm for ferrous, 399 nm for ferric, and 411 nm for ferrous−CO. These values are outside the ranges of the Soret maxima for ferrous, ferric, and ferrous−CO *b* cytochromes possessing a proximal histidine ligand (such as myoglobin and horseradish peroxidase), which are at 433−437, 403−410, and 420−423 nm, respectively (Mino et al., 1988). These differences are indicative of a change in the heme environment in the H25A mutant of hHO-1C$^-$ and imply that His25 is the proximal ligand for the HO-1 heme oxygenase. Resonance Raman data provide strong evidence for the loss of proximal histidine ligation in the heme−H25A complex (see below).

(B) Resonance Raman Spectroscopy of Ferrous Heme Complexes. For the ferrous 5-coordinate hemoproteins with a proximal histidine, the Fe−N(His) stretching vibration can be directly observed with 441.6-nm Soret excitation. The low-frequency resonance Raman spectra of the ferrous heme−hHO-1C$^-$ and heme−H25A complexes are presented in Figure 2. The Fe−N(His) stretching band at 216 cm^{-1} dominates in the wild-type heme oxygenase (hHO-1C$^-$) spectrum. This frequency is characteristic of a neutral imidazole ligand and is identical to that of rHO-1C$^-$ (Sun et al., 1993). The assignment of the ν[Fe−N(His)] band has

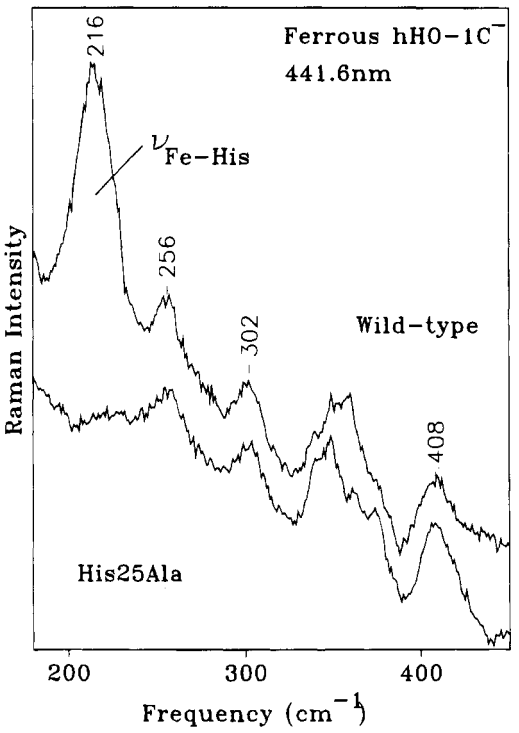

FIGURE 2: Resonance Raman spectra of Fe(II)PP−hHO-1C⁻ (top trace, ~200 μM, pH 7.4) and Fe(II)PP−His25Ala hHO-1C⁻ (bottom trace, ~250 μM, pH 7.4). Both are obtained with 441.6-nm excitation (20 mW at the sample).

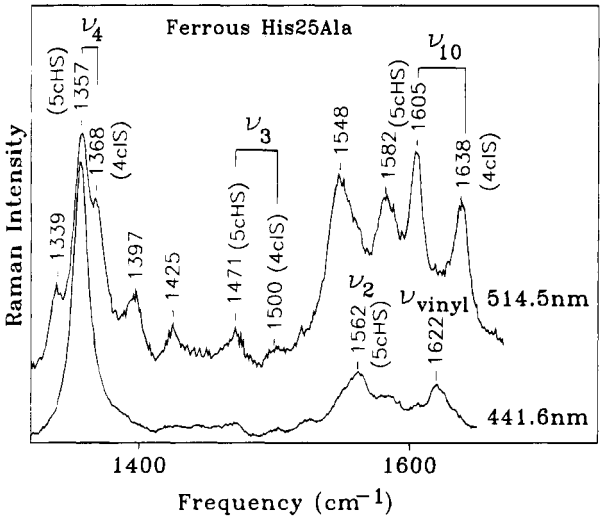

FIGURE 3: Resonance Raman spectra of Fe(II)PP−His25Ala hHO-1C⁻. Enzyme concentration was ~250 μM (pH 7.4). Laser power was 20 mW for 441.6-nm excitation and 45 mW for 514.5-nm excitation.

now been firmly established from the iron-isotope sensitivity of this peak, which these workers report as 218 cm^{-1} (Takahashi et al., 1994b). Point mutation of His 25 to Ala eliminates this intense band from the ferrous heme−H25A HO spectrum (Figure 2). This alteration provides compelling evidence that histidine is lost as an axial heme ligand in the mutant and, furthermore, identifies His 25 as the proximal ligand for the wild-type HO-1 heme oxygenase.

The resonance Raman spectra in the high-frequency region of the ferrous heme−H25A complex obtained with near-Soret (441.6 nm) and Q-band (514.5 nm) excitation are presented in Figure 3. (Excitation at 413.1 nm within the Soret absorption yields a spectrum very similar to that shown for 441.6-nm excitation.) These Soret-excited resonance Raman spectra are dominated by bands characteristic of a 5-coordinate high-spin ferrous hemoprotein (Spiro & Strekas, 1974; Rakshit & Spiro, 1974; Choi et al., 1982; Mino et al., 1988; Dasgupta et al., 1989; Palaniappan & Terner, 1989; Mylrajan et al., 1990). These bands include porphyrin skeletal modes at 1562 (ν_2), 1471 (ν_3), and 1357 (ν_4) cm^{-1}. As expected, the Q-band excitation at 514.5 nm leads to the observation of additional porphyrin skeletal modes of this 5-coordinate high-spin species at 1605 (ν_{10}) and 1548 cm^{-1} (ν_{11}). Another set of Raman frequencies is also observed with 514.5-nm excitation. The frequencies of these new bands (1368, 1500, and 1638 cm^{-1}) are characteristic for 4-coordinate intermediate-spin ferrous hemes (Andersson et al., 1992, 1989). For example, the band at 1638 cm^{-1} (depolarized) can only be assigned to ν_{10} of the 4-coordinate species for the ferrous hemes. Similarly, the band at 1368 cm^{-1} is not likely to be due to a ferrous heme other than a 4-coordinate species. Interestingly, a *6-coordinate, low-spin ferric heme* would show similar ν_4 and ν_{10} frequencies (Andersson et al., 1992). This circumstance could arise for the present case only if reduction were incomplete, and two strong-field axial ligands were present. Neither situation is probable nor indicated by the UV−vis spectrum. Furthermore, we show below that the resonance Raman spectrum of *ferric* heme−H25A obtained with 514.5-nm excitation *does not* contain bands at 1368, 1500, and 1638 cm^{-1}; its spectrum is completely characteristic of a 5-coordinate high-spin ferric heme. Therefore, the Raman bands at 1368, 1500, and 1638 cm^{-1} in the ferrous heme−H25A protein complex (Figure 3) are an unambiguous indication of the presence of a 4-coordinate ferrous heme species.

The UV−vis spectrum of the ferrous heme−H25A complex (Figure 1A), however, is indicative of predominantly 5-coordinate high-spin species. This is because the UV−vis bands of the 4-coordinate intermediate-spin species (Sage et al., 1991) are not discernible. The 4-coordinate species detected by resonance Raman spectroscopy is not likely to be produced dynamically by laser-induced photodissociation of the proximal ligand because its population does not appear to increase as a function of higher laser power. Furthermore, photodissociation of the proximal ligand has not been documented for hemoproteins under Q-band excitation. The presence of an equilibrium mixture in the ferrous heme−H25A complex at pH 7.4 of a smaller, but readily detectable, population of the 4-coordinate species and the dominant 5-coordinate species implies that the bond strength of the as yet unidentified axial ligand in the pentacoordinate complex is weak.

(C) Resonance Raman Spectroscopy of Ferric Heme Complexes. The resonance Raman spectrum (413.1-nm excitation, data not shown) of the ferric heme−hHO-1C⁻ complex is very similar to that of the heme−rHO-1C⁻ complex, which consists of a 6-coordinate high-spin/low-spin mixture (Sun et al., 1993). The sixth ligand in rHO-1C⁻ has been proposed to be a water molecule or an OH^-, depending on solution pH (Sun et al., 1993; Takahashi et al., 1994b). In contrast, the resonance Raman spectra of the ferric heme−H25A heme oxygenase complex are significantly different from those of the wild-type enzyme. The frequencies of the porphyrin skeletal modes (1570, 1491, 1372, 1628, ~1554, and 1570 cm^{-1} for ν_2, ν_3, ν_4, ν_{10}, ν_{11},

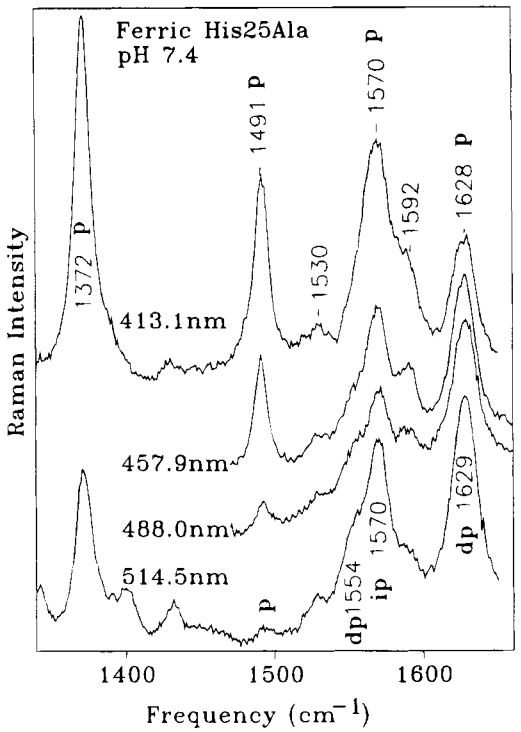

FIGURE 4: Resonance Raman of Fe(III)PP−His25Ala hHO-1C$^-$. ~200 μM enzyme in phosphate (pH 7.4) buffer. Excitation laser lines: 413.1 nm (25 mW), 457.9 nm (45 mW), 488.0 nm (45 mW), 514.5 nm (45 mW).

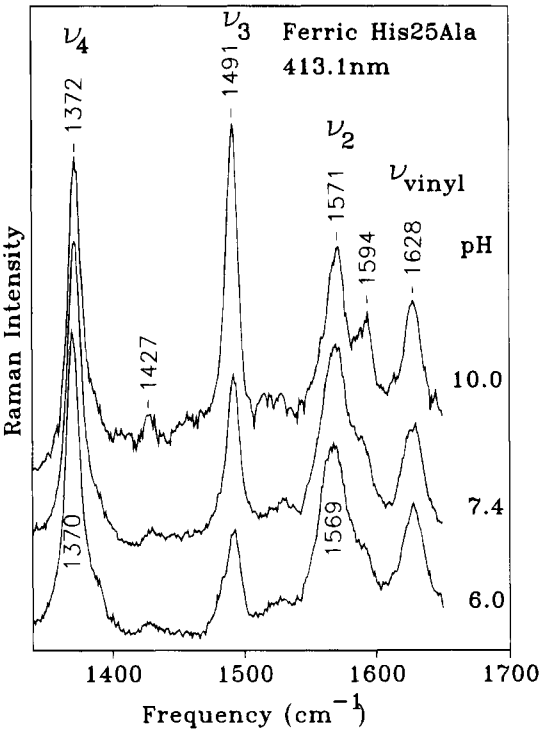

FIGURE 5: Resonance Raman of Fe(III)PP−His25Ala hHO-1C$^-$ obtained with 413.1-nm excitation (25 mW). ~200 μM enzyme in CAPS (pH 10.0), phosphate (pH 7.4), and MES (pH 6.0) buffers, respectively.

and ν_{19}, respectively) are characteristic for a 5-coordinate high-spin heme (Figure 4; Palaniappan & Terner, 1989; Smulevich et al., 1988a; Asher & Schuster, 1979; Egawa et al., 1993; Evangelista-Kirkup et al., 1985).

These frequencies for the ferric heme−H25A complex are almost independent of pH in the range from 6.0 to 10.0 (Figure 5). However, relative intensities do change with pH. Most strikingly, with 413.1-nm excitation of the pH 10.0 sample, the intensity of ν_3 at 1491 cm^{-1} is greater than that of ν_4 at 1372 cm^{-1}; this pattern is unprecedented in resonance Raman spectra of heme proteins and model compounds. With Soret excitation, ν_4 is usually the dominant Raman feature because its eigenvector matches the phasing of the electronic excited state $e_g^*(\pi)$ (Li et al., 1990). The phenomenon observed in this study is probably related to its unusual proximal ligation. The $e_g^*(\pi)$ orbital can interact with the iron $e_g(d_{xz},d_{yz})$ orbital, leading to π back-bonding from iron to the porphyrin ring. An unusual axial ligand can affect the energy level of iron $e_g(d_{xz},d_{yz})$, which modifies the energy level as well as the eigenvector of the $e_g^*(\pi)$ orbital. In fact, the significantly blue-shifted Soret absorption maximum for the ferric heme−H25A complex relative to other heme proteins can be explained with the increased interaction between the $e_g^*(\pi)$ and $e_g(d_{xz},d_{yz})$ orbitals. We have noticed that the relative intensity of ν_3 vs ν_4 of catalase, which has a proximal tyrosinate ligand, is much higher upon ~400-nm excitation than that in other heme proteins with proximal histidine ligands (Chuang et al., 1988; Sharma et al., 1989). The new proximal ligand in 5-coordinate H25A HO, however, is unlikely to be a tyrosinate. If a tyrosinate ligand were present, the characteristic tyrosinate side-chain vibrations, especially the one at ~1610 cm^{-1}, would be expected to have maximal enhancement with 488.0-nm excitation as observed in catalase (Chuang et al., 1988; Sharma et al., 1989) and in hemoglobin M mutants (Nagai et al., 1983; Nagai et al., 1989). No such band(s) is (are) observed in the resonance Raman spectra of the ferric heme−H25A complex (Q-excitations, Figure 4).

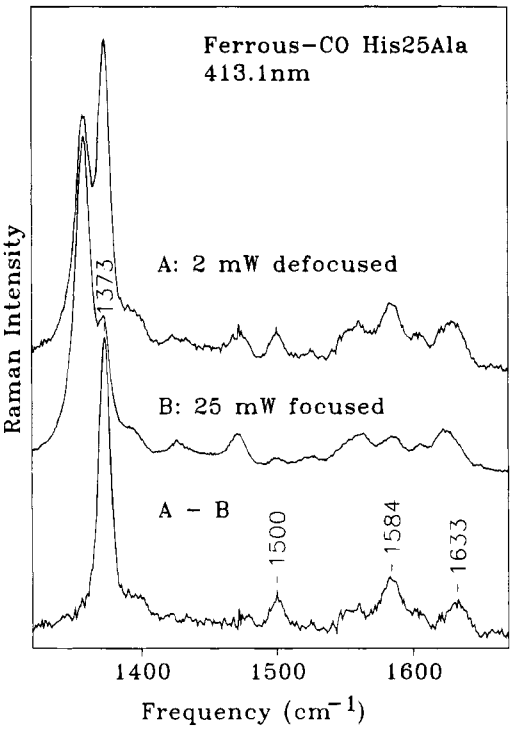

FIGURE 6: Resonance Raman spectra of the CO adduct of Fe(II)PP−His25Ala hHO-1C$^-$, obtained with 413.1-nm excitation. ~100 μM enzyme in phosphate buffer (pH 7.4). Different laser powers were used, as indicated.

(D) Carbonmonoxy Ferrous Heme−His25Ala HO Complex. To further explore the structural and electronic properties of the H25A mutant, we have investigated the

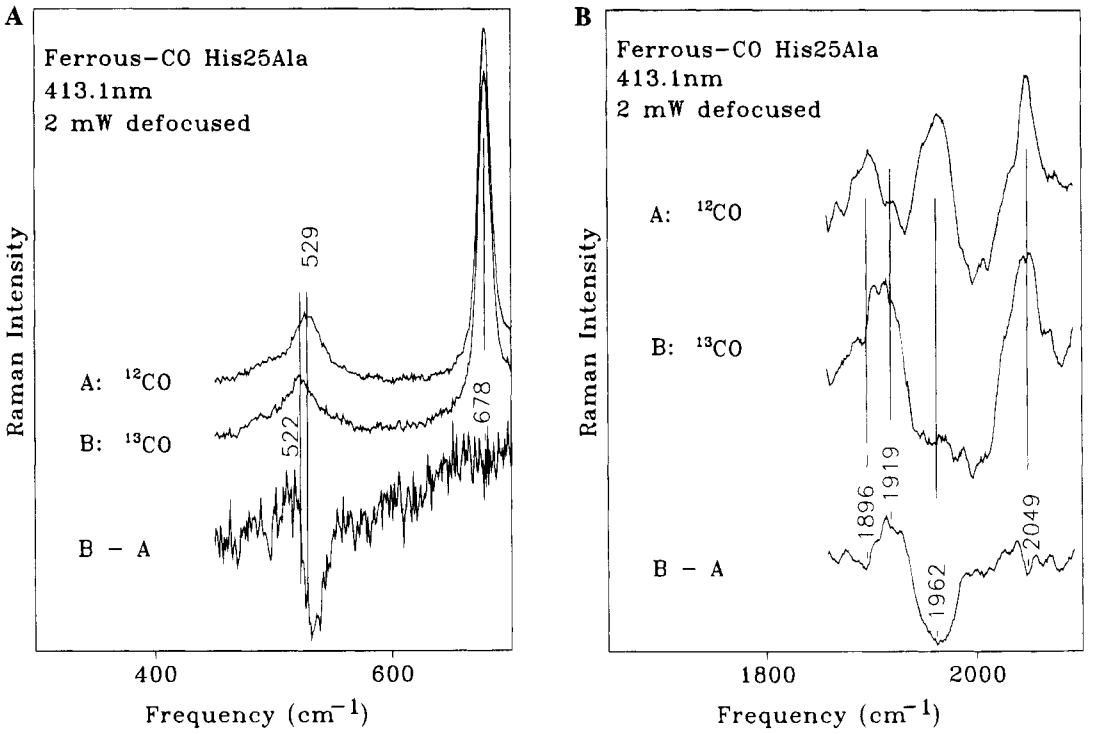

FIGURE 7: Resonance Raman spectra of the CO adduct of Fe(II)PP−His25Ala hHO-1C$^-$ obtained with 413.1-nm excitation. ~100 μM enzyme in phosphate buffer (pH 7.4). Laser power was 2 mW, and laser beam was slightly defocused at the sample. The spectra of the ^{12}CO and ^{13}CO adducts were recorded back-to-back. The traces in the high-frequency region (B) were subjected to a 17-point (Savitsky-Golay) smooth.

resonance Raman spectra of the CO adduct of ferrous heme−H25A complex. The high-frequency region obtained with 413.1-nm excitation is shown in Figure 6 and illustrates the dependence of the Raman spectrum on the laser power. This behavior is similar to that of CO·myoglobin and CO adducts of the other ferrous hemes. High laser power generally leads to the photodissociation of CO, resulting in the production of a 5-coordinate ferrous heme. In the present case, use of 25 mW of 413.1-nm laser irradiation gives a spectrum that is dominated by the bands characteristic of ferrous heme−H25A complex (Sun et al., 1993). Upon both reducing the laser power (to 2 mW) and defocusing the beam, the resonance Raman bands for CO-bound species are stronger than those of the photodissociated form, and spectral subtraction (low power − high power) yields the spectrum for the "pure" CO-bound species (Figure 6). Although photodissociation makes it more difficult to obtain a spectrum of the pure CO-bound species, it also facilitates the identification of bands associated with CO vibrations, because of the decrease in intensities of the C≡O stretching and Fe−CO stretching modes with increasing laser power. Such bands were found at 1962 and 529 cm^{-1} in the resonance Raman spectrum (Figure 7). (The FT-IR spectrum of a 300-μM sample showed a single prominent peak at 1959 cm^{-1}.) The former was easily identified as ν(C≡O) by its shift to 1919 cm^{-1} upon ^{13}CO substitution. The band at 529 cm^{-1} can be assigned to the ν(Fe−CO) stretching mode because of its shift to 522 cm^{-1} with ^{13}CO. (The calculated shift is 6.1 cm^{-1} for a diatomic oscillator model.) The intensity of the Fe−C−O bending mode was apparently too low to be observed in our samples. The CO-dependent frequencies, ν(C≡O), ν(Fe−CO), and δ(Fe−C−O), of the wild-type ferrous heme·CO complex of HO-1 were recently reported at 1958, 503, and 576 cm^{-1}, respectively (Takahashi et al., 1994b).

The carbonmonoxy adducts of heme proteins and model compounds have been extensively studied by resonance Raman spectroscopy (Uno et al., 1987; Yu & Kerr, 1988; Smulevich et al., 1988b; Ray et al., 1994). It has been found that the ν(C≡O) and ν(Fe−CO) frequencies exhibit an inverse relationship, that can be explained by the π back-bonding interaction between the iron $e_g(d_{xz},d_{yz})$ and the CO π^* orbital. Increased π back-bonding raises ν(Fe−CO) but lowers ν(C≡O). The degree of the π back-bonding is modulated by the nature of the proximal ligand (*trans* to CO) as well as the polarity and possible H-bonding interactions in the distal heme pocket, the site of CO binding. The ν(C≡O) and ν(Fe−CO) frequencies for a series of heme proteins are linearly correlated with a negative slope for species possessing the same proximal ligand. For example, *b* cytochromes with a proximal histidine ligand and cytochrome P-450 with a proximal cysteine thiolate ligand show such relationships. Any change in the proximal ligand, such as its state of ionization or degree of H-bonding, causes deviations from the inverse linear relationship. The polarity of the CO binding pocket determines the position of a heme protein along the correlation line. The position of the datum for the heme−H25A HO complex in the ν(C≡O) vs ν(Fe−CO) plot deviates very markedly from the line formed for heme proteins with a proximal histidine ligand (Ray et al., 1994). The direction of this deviation indicates that the proximal ligand for H25A is a *much weaker ligand than a histidine*. This result is fully consistent with the resonance Raman data of the ferrous heme−H25A complex described above. Moreover, the position of the heme−H25A HO complex in the plot also reveals that CO is located in a very hydrophobic pocket. The lack of resonance Raman intensity of the Fe−C−O bending mode for the heme−H25A complex should also be taken as evidence that the CO binding environment is hydrophobic, according to a recent proposal

(Ray at al., 1994). As a matter of fact, the CO and Fe−CO frequencies for the heme−H25A complex are almost the same as those of OC·FeDeut(THF) (1962 and 530 cm^{-1}) or OC·FeTpiv(THF) (1957 and 526 cm^{-1}), in which the proximal ligand is weak and the CO binding site is hydrophobic (Kerr et al., 1983; Kerr, 1984).

CONCLUSIONS

The UV−vis and resonance Raman data presented here provide evidence that His 25 is the proximal ligand in HO-1 heme oxygenase and facilitates binding of the heme substrate. Point mutation of histidine 25 to alanine produces a protein that is still capable of binding the heme substrate, but, in this case, with a new, very weak proximal ligand. In the ferric heme−H25A HO complex, the iron is in a high-spin, pentacoordinate state, whereas in the wild-type enzyme·substrate complex, it is six-coordinate (Sun et al., 1993). The reduced form of this complex exhibits a mixture of species. The smaller population appears to have a tetracoordinate ferrous heme devoid of axial ligands. The larger proportion has a high-spin, pentacoordinate ferrous heme. The exact identity of this new ligand in both the ferric and ferrous forms is unknown at this time. Although a histidine and a tyrosine are excluded as possibilities from the present resonance Raman data, the new ligand may come from a different amino acid side chain or even a water molecule. Moreover, the site of attachment (proximal or distal) of the new ligand is also unknown. [The only likely residues capable of donating a side-chain ligand in the vicinity of the original proximal His 25 or the distal His 132 are Glu 23 or Glu 29, and Glu 127, respectively (Yoshida et al., 1988).] Consequently, we also do not know the side of attachment of CO in the OC·Fe^{2+}(H25A)HO complex.

His 25 is known to be an essential residue for the activity of the enzyme (McCoubrey & Maines, 1993). The other essential histidine residue (His 132, rat liver enzyme) of the wild-type enzyme is located in the highly conserved 24 amino acid domain and had been previously thought to be a good candidate as the proximal histidine. However, in view of the new findings reported in this paper, its essential role is more likely to be that of a H-bond donor in the distal pocket, which channels oxygen specifically toward the α-meso carbon position. Additional work has suggested that His 132 may not be required for HO-1 heme oxygenase, although it is essential for HO-2 heme oxygenase activity (Takahashi et al., 1994a). We have proposed that the proximal side of the wild-type enzyme plays little role in the oxygen activation mechanism during heme degradation (Wilks & Ortiz de Montellano, 1993; Sun et al., 1993; Hernández et al, 1994). It is, therefore, not surprising that the distal pocket of the heme oxygenase should be highly conserved. We have obtained Raman spectroscopic evidence that the bound azide in the distal side of the wild-type enzyme is strongly H-bonded (Sun, Loehr, Wilks, and Ortiz de Montellano, unpublished results). NMR experiments reveal 5 exchangeable protons in the heme pocket. This highly conserved 24-amino acid domain contains more than 5 proton donors and is a good candidate to form the distal pocket (Hernández et al., 1994). We suspect that the weak proximal ligand in the H25A complex, although yet to be identified, is from this pocket. The CO binding site in the heme−H25A complex is very hydrophobic as judged from the ν(CO) vs ν(Fe−CO) plot, and might not be in the distal pocket of the wild-type enzyme. The investigation of the His132Ala mutant of hHO-1C^{-} is now in progress in our laboratories.

ACKNOWLEDGMENT

We thank Dr. Brian J. Reedy for help with the FT-IR data acquisition on the CO adduct of the heme−H25A complex.

REFERENCES

Andersson, L. A., Mylrajan, M., Sullivan, E. P., Jr., & Strauss, S. H. (1989) *J. Biol. Chem. 264*, 19099−19102.

Andersson, L. A., Mylrajan, M., Loehr, T. M., Sullivan, E. P., Jr., & Strauss, S. H. (1992) *New J. Chem. 16*, 569−576.

Asher, S. A., & Schuster, T. M. (1979) *Biochemistry 18*, 5377−5387.

Bonkovsky, H. L., Healey J. F., & Pohl, J. (1990) *Eur. J. Biochem. 189*, 155−166.

Choi, S., Spiro, T. G., Langry, K. C., Smith, K. M., Budd, D. L., & La Mar, G. N. (1982) *J. Am. Chem. Soc. 104*, 4345−4351.

Chuang, W.-J., Johnson, S., & Van Wart, H. E. (1988) *J. Inorg. Biochem. 34*, 201−219.

Dasgupta, S., Rousseau, D. L., Auni, H., & Yonetani, T. (1989) *J. Biol. Chem. 264*, 654−662.

Egawa, T., Kitagawa, T., & Makino, R. (1993) *Biochemistry 32*, 241−252.

Evangelista-Kirkup, R., Crisanti, M., Poulos, T. L., & Spiro, T. G. (1985) *FEBS Lett. 190*, 221−226.

Evans, C.-O., Healey, J. F., Greene, Y., & Bonkovsky, H. L. (1991) *Biochem. J. 273*, 659−666.

Hernández, G., Wilks, A., Paolesse, R., Smith, K. M., Ortiz de Montellano, P. R., & La Mar, G. N. (1994) *Biochemistry 33*, 6631−6641.

Ishikawa, K., Sato, M., Ito, M., & Yoshida, T. (1992) *Biochem. Biophys. Res. Commun. 182*, 981−986.

Kerr, E. A. (1984) Ph.D. Dissertation, Georgia Institute of Technology, Atlanta, GA.

Kerr, E. A., Mackin, H. C., & Yu, N.-T. (1983) *Biochemistry 22*, 4373−4379.

Li, X.-Y., Czernuszewicz, R. S., Kincaid, J. R., Stein, P. B., & Spiro, T. G. (1990) *J. Phys. Chem. 94*, 47−62.

Loehr, T. M., & Sanders-Loehr, J. (1993) *Methods Enzymol. 226*, 431−470.

Maines, M. D. (1988) *FASEB J. 2*, 2557−2568.

Maines, M. D. (1992) *Heme Oxygenase−Clinical Applications and Functions*, CRC Press, Boca Raton, FL.

Maines, M. D., Trakshel, G. M., & Kutty, R. K. (1986) *J. Biol. Chem. 261*, 411−419.

McCoubrey, W. K., Jr., & Maines, M. D. (1993) *Arch. Biochem. Biophys. 302*, 402−408.

Mino, Y., Wariishi, H., Blackburn, N., Loehr, T. M., & Gold, M. H. (1988) *J. Biol. Chem. 263*, 7029−7036.

Mylrajan, M., Valli, K., Wariishi, H., Gold, M. H., & Loehr, T. M. (1990) *Biochemistry 29*, 9617−9623.

Nagai, M., Kagimoto, T., Hayashi, A., Taketa, F., & Kitagawa, T. (1983) *Biochemistry 22*, 1305−1311.

Nagai, M., Yoneyama, Y., & Kitagawa, T. (1989) *Biochemistry 28*, 2418−2422.

Palaniappan, V., & Terner, J. (1989) *J. Biol. Chem. 264*, 16046−16053.

Rakshit, G., & Spiro, T. G. (1974) *Biochemistry 13*, 5317−5323.

Ray, G. B., Li, X.-Y., Ibers, J. A., Sessler, J. L., & Spiro, T. G. (1994) *J. Am. Chem. Soc. 116*, 162−176 and references therein.

Sage, J. T., Morikis, D., & Champion, P. M. (1991) *Biochemistry 30*, 1227−1237.

Sharma, K. D., Andersson, L. A., Loehr, T. M., Terner, J., & Goff, H. M. (1989) *J. Biol. Chem. 264*, 12772−12779.
Shibahara, S., Müller, R., Taguchi, H., & Yoshida, T. (1985) *Proc. Natl. Acad. Sci. U.S.A. 82*, 7865−7869.
Smulevich, G., Mauro, J. M., Fishel, L. A., English, A. M., Kraut, J., & Spiro, T. G. (1988a) *Biochemistry 27*, 5477−5485.
Smulevich, G., Mauro, J. M., Fishel, L. A., English, A. M., Kraut, J., & Spiro, T. G. (1988b) *Biochemistry 27*, 5486−5492.
Spiro, T. G., & Strekas, T. C. (1974) *J. Am. Chem. Soc. 96*, 338−345.
Stevens, C. F., & Wang, Y. (1993) *Nature 364*, 147−148.
Sun, J., Wilks, A., Ortiz de Montellano, P. R., & Loehr, T. M. (1993) *Biochemistry 32*, 14151−14157.
Takahashi, S., Wang, J., Rousseau, D. L., Ishikawa, K., Yoshida, T., Host, J. R., & Ikeda-Saito, M. (1994a) *J. Biol. Chem. 269*, 1010−1014.
Takahashi, S., Wang, J., Rousseau, D. L., Ishikawa, K., Yoshida, T., Takeuchi, N., & Ikeda-Saito, M. (1994b) *Biochemistry 33*, 5531−5538.
Tenhunen, R., Marver, H. S., & Schmid, R. (1969) *J. Biol. Chem. 244*, 6388−6394.
Uno, T., Nishimura, Y., Tsuboi, M., Makino, R., Iizuka, T., & Ishimura, Y. (1987) *J. Biol. Chem. 262*, 4549−4556.
Verma, A., Hirsch, D. J., Glatt, C. E., Ronnett, G. V., & Snyder, S. H. (1993) *Science 259*, 381−384.
Wilks, A., & Ortiz de Montellano, P. R. (1993) *J. Biol. Chem. 268*, 22357−22362.
Yoshida, T., & Kikuchi, G. (1978) *J. Biol. Chem. 253*, 4224−4229.
Yoshida, T., & Kikuchi, G. (1979) *J. Biol. Chem. 254*, 4487−4491.
Yoshida, T., Biro, P., Cohen, T., Müller, R., & Shibahara, S. (1988) *Eur. J. Biochem. 171*, 457−461.
Yoshinaga, T., Sassa, S., & Kappas, A. (1982) *J. Biol. Chem. 257*, 7778−7785.
Yu, N.-T., & Kerr, E. A. (1988) in *Biological Applications of Raman Spectroscopy* (Spiro, T. G., Ed.) Vol. 3, pp 39−95, Wiley, New York.
Zhuo, M., Small, S. A., Kandel, E. R., & Hawkins, R. D. (1993) *Science 260*, 1946−1950.